Journal of Cardiovascular Magnetic Resonance (2007) **9,** 687–695

ISSN: 1097-6647 print / 1532-429X online
DOI: 10.1080/10976640601187596

informa
healthcare

Variations in Right Ventricular Outflow Tract Morphology Following Repair of Congenital Heart Disease: Implications for Percutaneous Pulmonary Valve Implantation

Silvia Schievano,[1] Louise Coats,[1] Francesco Migliavacca,[2] Wendy Norman,[1] Alessandra Frigiola,[1] John Deanfield,[1] Philipp Bonhoeffer,[1] and **Andrew M. Taylor[1]**

UCL Institute of Child Health and Great Ormond Street Hospital for Children, London, United Kingdom[1]
Laboratory of Biological Structure Mechanics, Structural Engineering Department, Politecnico di Milano, Milan, Italy[2]

ABSTRACT

Objective: **Our aim was to identify sub-groups of right ventricular outflow tract morphology that would be suitable for percutaneous pulmonary valve implantation and to document their prevalence in our patient population.** ***Materials and Methods:*** **Eighty-three consecutive patients with right ventricular outflow tract dysfunction (5–41 years, 76% tetralogy of Fallot) referred to our center for cardiovascular magnetic resonance were studied. A morphological classification was created according to visual assessment of three-dimensional reconstructions and detailed measurement. Diagnosis, right ventricular outflow tract type, surgical history and treatment outcomes were documented.** ***Results:*** **Right ventricular outflow tract morphology was heterogeneous; nevertheless, 5 patterns were visually identified. Type I, a pyramidal morphology, was most prevalent (49%) and related to the presence of a transannular patch. Other types (II–V) were seen more commonly in patients with conduits. Two patients had unclassifiable morphology. Ninety-five percent of patients were assigned to the correct morphological classification by visual assessment alone. Percutaneous pulmonary valve implantation was performed successfully in 10 patients with Type II–V morphology and in 1 patient with unclassifiable morphology. Percutaneous implantation was not performed in patients with Type I morphology. Only right ventricular outflow tract diameters $<$22 mm in diameter were suitable for the current device.** ***Conclusions:*** **We have created a morphological classification of the RVOT in patients referred for assessment of RVOT dysfunction. Though only 13% of our patients underwent percutaneous implantation, $>$50% of outflow tract morphologies may be suitable for this approach, in particular with the development of new devices appropriate for larger outflow.**

Keywords: Right ventricular outflow tract, 3D reconstruction, transcatheter, pulmonary valve implantation.
The authors would like to thank Matthew Fenton and Johannes Nordmeyer for their help with the statistical analysis.
Correspondence to:
Silvia Schievano
Cardiothoracic Unit
UCL Institute of Child Health and
Great Ormond Street Hospital for Children
Great Ormond Street
London WC1N 3JH
UK
tel: +44 2078138106; fax: +44 2078138262
email: s.schievano@ich.ucl.ac.uk.

INTRODUCTION

Substantial progress in surgical techniques for repairing complex congenital heart defects has resulted in increasing numbers of patients surviving into adulthood (1). The focus has now shifted towards treatment of morbidity, with pathology of the pulmonary valve being one of the most common conditions that requires intervention (2–5). However, enthusiasm for repeated surgery is tempered by the limited longevity of surgically implanted valves or conduits (6). For those with obstructed outflow tracts, bare stenting can delay surgery but at the cost of pulmonary regurgitation (7).

Recently, we have introduced a novel procedure that can relieve both regurgitation and/or stenosis in the right ventricular outflow tract (RVOT) by a minimally invasive approach

(8, 9). Percutaneous pulmonary valve implantation (PPVI) involves transcatheter placement of a valved stent within the existing degenerated valve or conduit and can be performed without cardiopulmonary bypass or residual pulmonary regurgitation. Selection of patients for this exciting new technique depends on the presence of an appropriate site for implantation within the RVOT that will ensure device stability. The currently available device is composed of a bovine jugular venous valve sutured into a balloon-expandable platinum-iridium stent. It has an unexpanded length of 35 mm and can be deployed to a maximum diameter of 22 mm. The diameter of deployment is determined by the balloon size of the delivery system.

Cardiovascular magnetic resonance (CMR) can assess three-dimensional (3D) morphology in patients with congenital heart disease without exposure to x-rays (10). The aim of this study was to identify sub-groups of RVOT morphology that would be suitable for PPVI and to document their prevalence in our patient population.

MATERIALS AND METHODS

Study population

We retrospectively studied 83 consecutive patients with RVOT dysfunction, following previous repair of congenital heart disease, who were referred to our institution for CMR between March 2003 and February 2005. Clinical indications for PPVI mirror the conventional criteria for surgical re-intervention and include pulmonary regurgitation with increasing right ventricular size, substantial tricuspid regurgitation, arrhythmia and/or impairment in exercise capacity or RVOT obstruction with right ventricular pressure greater than 2/3 systemic. Patients <5 years old were not included as they are currently unsuitable for PPVI on account of size alone. Patient characteristics are shown in Table 1. Institutional ethical approval for CMR was obtained and all subjects (and/or a parent/guardian) gave informed consent for retrospective data analysis of the CMR images.

Table 1. Patient characteristics

Category	n	%
Gender		
Male	45	(54.2)
Female	38	(45.8)
Age at scan		
5–12 years	30	(36.1)
12–18 years	38	(45.8)
>18 years	15	(18.1)
Primary diagnosis		
Tetralogy of Fallot	40	(48.2)
Pulmonary atresia	19	(22.9)
Truncus arteriosus	7	(8.4)
Transposition of the great arteries	6	(7.2)
Pulmonary stenosis	5	(6.0)
Double outlet right ventricle	4	(4.8)
Other	2	(2.4)
RVOT type		
Transannular patch	40	(48.2)
Homograft	23	(27.7)
Native	9	(10.8)
RVOT patch	8	(9.6)
Other	3	(3.6)
Open operations		
1	67	(80.7)
2	13	(15.7)
3	2	(2.4)
4	1	(1.2)

RVOT = right ventricular outflow tract.

Cardiovascular magnetic resonance

CMR was performed at 1.5T (Symphony–Maestro class, Siemens Medical Systems, Erlangen, Germany) using a 4-element body phased array coil. Pulmonary artery through-plane flow data was acquired using a flow sensitive gradient echo sequence (TR 8ms, TE 3.8 ms, flip angle 30°, 3 averages, parallel imaging (iPAT) factor 2, resolution 1.3 × 1.3 × 5 mm) and retrospective cardiac gating during free breathing. A phase correction filter was used to correct for phase errors introduced by eddy currents and Maxwell terms. The image plane was located at the midpoint of the pulmonary trunk (11). Pulmonary flow and velocity was calculated from the phase contrast images using a semi-automatic vessel edge detection algorithm with operator correction. Regurgitant fraction was calculated as the percent backward flow over forward flow. A 3D gradient echo sequence was used to acquire the MR angiography after the administration of 0.4 mL/kg of Gadolinium–imaging parameters: TR 3.7 ms, TE 1.4 ms, flip angle 25°, resolution 1.3 × 0.8 × 1.3 mm. The raw DICOM data of the patient's MR angiogram were imported into image processing software for 3D reconstruction.

Three-dimensional reconstruction

Reconstruction from MR images was performed using the image processing package Mimics (Materialise Inc., Ann Arbor, Michigan, USA). Segmentation and editing tools were used to detect the region of interest, the RVOT, in three two-dimensional orthogonal planes (axial, coronal and sagittal). We have previously demonstrated the accuracy of this method at our Institution (12). When the region of interest was completely separated from the adjacent structures, the software calculated a 3D volume of the inner wall of the RVOT by means of pattern recognition and interpolation algorithms (Fig. 1) (12).

Three-dimensional volume analysis

Mimics software enables rotation and scaling of 3D objects. This allows complete appreciation of the 3D RVOT anatomy. First, a morphological classification was created based on visualization of the patients' RVOT alone (AMT). Five types of RVOT morphology were identified (Fig. 2). Type I had a pyramidal shape (wide proximally and narrow distally). Type II had a constant diameter. Type III had an inverted pyramidal shape (narrow proximally and wide distally), Type IV was wide centrally but narrowed proximally and distally. Type V was narrowed centrally but wide proximally and distally.

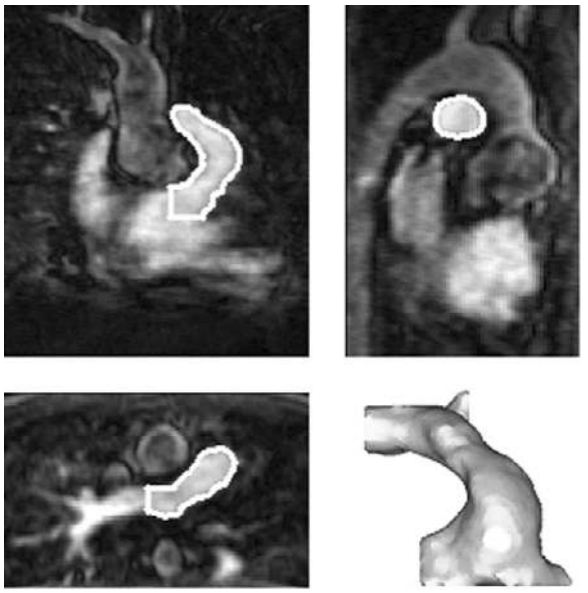

Figure 1. Two-dimensional CMR (coronal, sagittal and axial planes) and 3D RVOT reconstructed volume.

The center axis of the 3D RVOT volume was identified and, starting from the pulmonary bifurcation, divided into 10 mm segments. The RVOT volume was then sectioned by planes orthogonal to the center axis at each of these points. The perimeter of each of these sections was measured, and the shape of the cross-sectional area standardized to a circle. During PPVI, pressure inflation of the balloon deploying the device usually achieves a cylindrical configuration. It is, therefore, the diameter of this final circle which will influence stability of the device, resulting in a successful procedure. The diameter of these circles was measured and graphically represented against the length of the RVOT, standardized in order to visualize the morphology independent from length (Fig. 3).

Each morphological type was defined mathematically (SS).

The diameters, y_A, and y_C, were measured at 0% and 100% of the RVOT length, respectively, for all morphological types. The diameter, y_B, was measured at 50% of the RVOT length in patients with Type I, II or III morphology. In patients with Types IV morphology, y_B was measured at the point of maximum diameter irrespective of its position along the length of the RVOT. In Type V morphology, y_B was measured at the point of minimum diameter. The average diameter $\bar{y}$ along the RVOT length was determined. The difference between diameters were calculated and expressed as a percentage of the average RVOT diameter.

$$\Delta y_1 = \frac{y_B - y_A}{\bar{y}} \cdot 100 \qquad [1]$$

and

$$\Delta y_2 = \frac{y_C - y_B}{\bar{y}} \cdot 100. \qquad [2]$$

The mathematical rules defining each morphological type are described by the following systems and use the two unknowns Δy_1 and Δy_2:

$$\text{Type I}: \begin{cases} \Delta y_1 > -10\% \\ \Delta y_2 > -10\% \\ \Delta y_1 + \Delta y_2 > 10\% \vee \Delta y_1 > 10\% \vee \Delta y_2 > 10\% \end{cases} \qquad [3]$$

$$\text{Type II}: \begin{cases} -10\% \leq \Delta y_1 \leq 10\% \\ -10\% \leq \Delta y_2 \leq 10\% \\ -10\% \leq \Delta y_1 + \Delta y_2 \leq 10\% \end{cases} \qquad [4]$$

$$\text{Type III}: \begin{cases} \Delta y_1 < 10\% \\ \Delta y_2 < 10\% \\ \Delta y_1 + \Delta y_2 < -10\% \vee \Delta y_1 < -10\% \vee \Delta y_2 < -10\% \end{cases} \qquad [5]$$

$$\text{Type IV}: \begin{cases} \Delta y_1 > 10\% \\ \Delta y_2 < -10\% \end{cases} \qquad [6]$$

$$\text{Type V}: \begin{cases} \Delta y_1 < -10\% \\ \Delta y_2 > 10\% \end{cases} . \qquad [7]$$

The above mathematical descriptions are graphically presented in Figure 4.

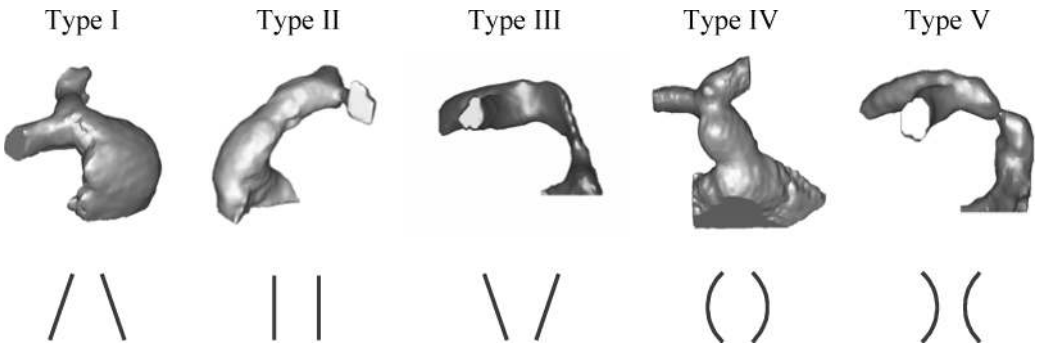

Figure 2. Five types of RVOT morphology.

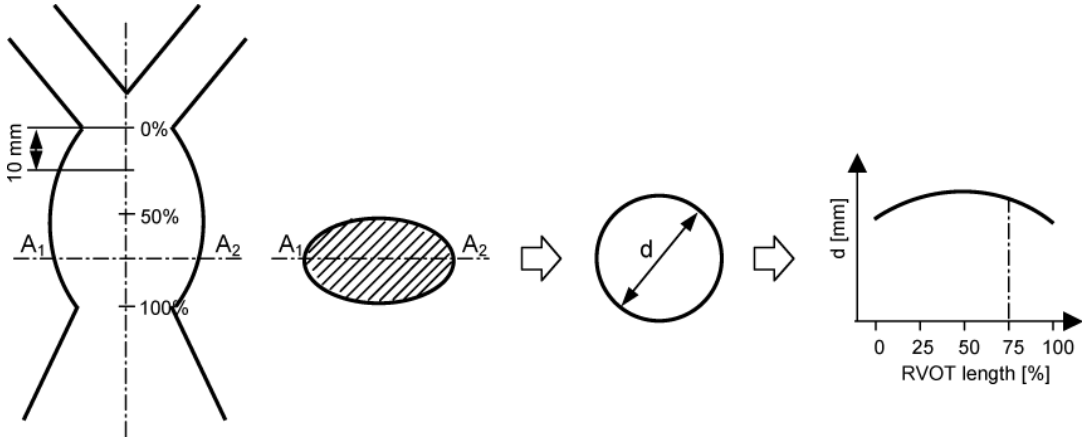

Figure 3. Mathematical volume analysis. The perimeter of each section of the RVOT is standardized to a circle. The diameter (d) of the circle is measured and graphically represented against the length of the RVOT.

Statistical analysis

All categorical variables were expressed as an absolute number and a percentage. Comparison between categories and calculation of the odds ratio were made using the Fisher's exact test. Significance was accepted if $p < 0.05$ with 95% confidence intervals.

RESULTS

Three-dimensional volume analysis

RVOT anatomy was heterogeneous. Five common types were identified (Fig. 2). On the basis of visual assessment, 44.6% (37/83 patients) were assigned to type I, 16.9% (14/83) to type II,

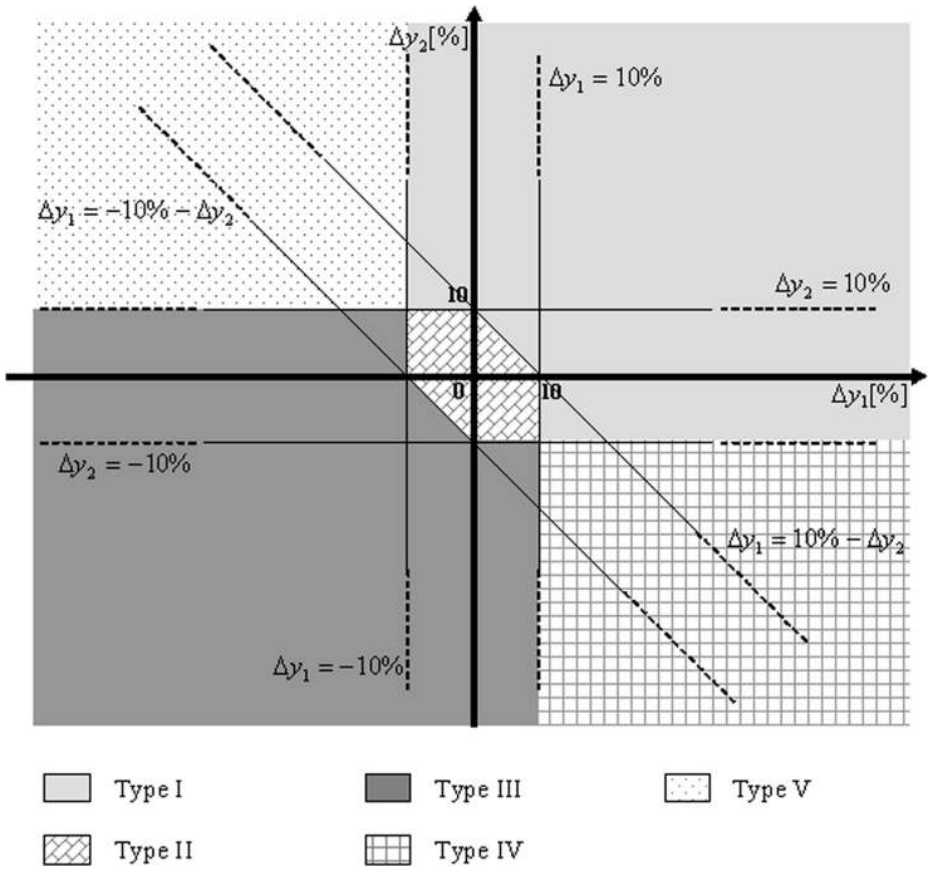

Figure 4. Graphical representation of the systems' solutions which mathematically describe the 5 morphological types.

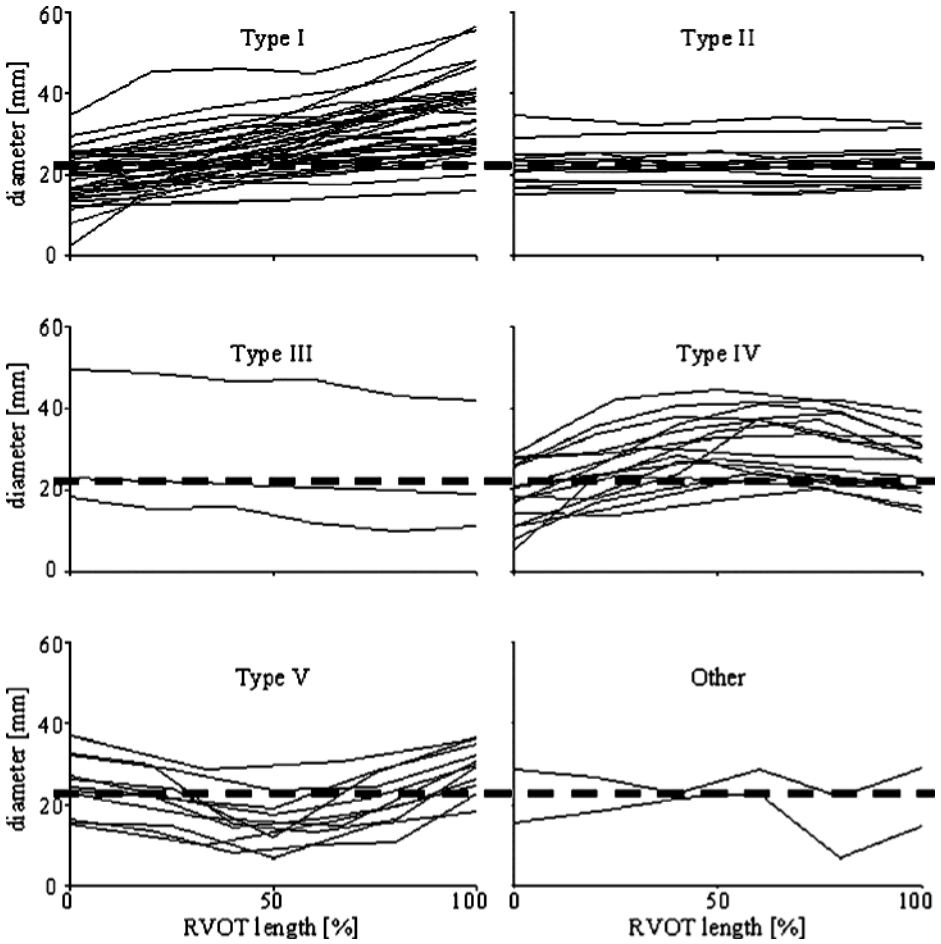

Figure 5. RVOT profiles divided by morphological types and standardized along RVOT length. Only RVOT diameters <22 mm (dashed lines) are suitable for the current PPVI device.

3.6% (3/83) to type III, 19.3% (16/83) to type IV and 13.3% (11/83) to type V. 2.4% (2/83) of patients could not be classified into any of these types. However, when mathematical analysis and standardization of length was applied (Fig. 5), 4.8% (4/83) of patients were reclassified; 2 patients from type II and 2 from type IV were moved to type I (Table 2). The distribution of the classifiable patients ($n = 81$) in the $\Delta y_1 \Delta y_2$ coordinate system is shown in Figure 6.

Clinical correlates

The majority of patients in our population had tetralogy of Fallot and the commonest outflow tract was a transannular patch. The prevalence of different diagnoses and RVOT types is shown in Table 2. No direct correlation was found between surgical history or underlying diagnosis and morphological type. Transannular patch was more commonly seen in patients with type I morphology compared to those with types II–V (Fig. 7a, Odds Ratio 0.28, $p < 0.05$). Furthermore, type I morphology was associated with a higher regurgitant fraction than types II–V (Fig. 7b, Odds Ratio 0.33, $p < 0.05$).

Eleven patients underwent PPVI: 2 patients with type II morphology, 2 with type III, 3 with type IV and 3 with type V and 1 patient whose morphology was unclassifiable. All had a homograft outflow tract, and none had type I morphology which was felt unsuitable because of the risk of proximal device dislodgement.

Twelve patients had homograft outflow tracts but did not undergo PPVI. Homograft outflow tracts are often appropriate for PPVI because of their circumferential nature and tendency to calcify and comprise much of the clinical experience (9). Importantly, however, 6 patients in this population had homograft conduits with type I morphology and thus were unsuitable for PPVI with the current device. These patients represent 26% (6/23) of all those with homograft conduits in our patient population. Three patients had insufficient valvar/conduit dysfunction to warrant intervention to the RVOT, but all had stents placed to treat branch pulmonary artery stenosis. Two patients underwent surgery as PPVI was not widely available at the time of their referral. One patient was followed-up medically as there was no clinical indication for intervention.

Table 2. Summary of results

Category	I	II	III	IV	V	Other	Total
n	41 (49.4)	12 (14.5)	3 (3.6)	14 (16.9)	11 (13.3)	2 (2.4)	83
Peak velocity (m/s)							
≤ 2	22 (53.7)	7 (58.3)	3 (100.0)	9 (64.3)	6 (54.5)	1 (50.0)	48
>2 and ≤3	10 (24.4)	3 (25.0)	0 (0.0)	2 (14.3)	1 (9.1)	1 (50.0)	17
>3	9 (22.0)	2 (16.7)	0 (0.0)	3 (21.4)	4 (36.4)	0 (0.0)	18
Regurgitation fraction							
mild (≤20%)	7 (7.3)	4 (33.3)	2 (33.3)	3 (21.4)	6 (36.4)	1 (0.0)	23
moderate or severe (>20%)	34 (17.1)	8 (33.3)	1 (66.7)	11 (21.4)	5 (54.5)	1 (50.0)	60
Primary diagnosis							
Tetralogy of Fallot	25 (61.0)	4 (33.3)	0 (0.0)	8 (57.1)	3 (27.3)	0 (0.0)	40
Pulmonary atresia	7 (17.1)	4 (33.3)	0 (0.0)	3 (21.4)	3 (27.3)	2 (100.0)	19
Truncus arteriosus	1 (2.4)	1 (8.3)	1 (33.3)	1 (7.1)	3 (27.3)	0 (0.0)	7
Transposition of the great arteries	3 (7.3)	2 (16.7)	0 (0.0)	0 (0.0)	1 (9.1)	0 (0.0)	6
Pulmonary stenosis	2 (4.9)	1 (8.3)	1 (33.3)	0 (0.0)	1 (9.1)	0 (0.0)	5
Double outlet right ventricle	2 (4.9)	0 (0.0)	0 (0.0)	2 (14.3)	0 (0.0)	0 (0.0)	4
Other	1 (2.4)	0 (0.0)	1 (33.3)	0 (0.0)	0 (0.0)	0 (0.0)	2
RVOT type							
Transannular patch	25 (61.0)	5 (41.7)	0 (0.0)	6 (42.9)	4 (36.4)	0 (0.0)	40
Homograft	6 (14.6)	4 (33.3)	2 (66.7)	4 (28.6)	6 (54.5)	1 (50.0)	23
Native	3 (7.3)	2 (16.7)	1 (33.3)	1 (7.1)	1 (9.1)	1 (50.0)	9
RVOT patch	4 (9.8)	1 (8.3)	0 (0.0)	3 (21.4)	0 (0.0)	0 (0.0)	8
Other	3 (7.3)	0 (0.0)	0 (0.0)	0 (0.0)	0 (0.0)	0 (0.0)	3
Procedure							
Surgery	30 (73.2)	5 (41.7)	0 (0.0)	3 (21.4)	4 (36.4)	0 (0.0)	42
PPVI	0 (0.0)	2 (16.7)	2 (66.7)	3 (21.4)	3 (27.3)	1 (50.0)	11
Other percutaneous	3 (7.3)	1 (8.3)	0 (0.0)	1 (7.1)	0 (0.0)	1 (50.0)	6
Surgery + other percutaneous	1 (2.4)	0 (0.0)	0 (0.0)	0 (0.0)	1 (9.1)	0 (0.0)	2
No intervention	7 (17.1)	4 (33.3)	1 (33.3)	7 (50.0)	3 (27.3)	0 (0.0)	22

PPVI = percutaneous pulmonary valve implantation, RVOT = right ventricular outflow tract.

DISCUSSION

This study, for the first time, characterizes the spectrum of RVOT morphology that is present in patients late after surgical repair of congenital heart disease. Although this group often appears heterogeneous, five common RVOT types can be described by simple mathematical rules. Morphology of the RVOT is a major determinant of suitability for PPVI, highlighting the importance of 3D imaging in patient assessment and selection.

Type I morphology, a pyramidal shape, occurred in 49% of patients. This morphology was associated with a transannular patch repair and is unsuitable for percutaneous valve intervention with the current device, as implanted prostheses would have a high probability of migrating proximally. Importantly, some patients with transannular patches had type II–V morphology and may be amenable, whilst conversely a quarter of those with homografts, who we conventionally regard as good candidates, had unsuitable type I RVOT morphology. Whilst surgical history can suggest suitability for PPVI, it does not, therefore, identify adequately all patients with appropriate morphology. Three dimensional characterization of the RVOT using CMR or computerized tomography provides important complementary information when selecting patients for PPVI or other minimally invasive approaches to treat RVOT dysfunction (13).

From a morphological perspective, we could have attempted PPVI in all types of RVOT except the pyramidal type (type I). In fact, we only performed PPVI in 11 patients from 42 with suitable morphologies, as other factors influence patient selection for this procedure. The current clinical device is only suitable for those patients whose outflow tracts are <22 mm in diameter in our Institution. The development of larger devices and new device designs that permit downsizing of dilated outflow tracts to the size of biologically available valves is underway and will increase the number of patients that could benefit from a percutaneous approach in the future (13).

Further important considerations are the compliance of the RVOT and movement of the RVOT/ pulmonary trunk junction (e.g., due to strain in the tissues caused by attachment to the ventricles), which are not assessed by CMR angiography. A patient with type II-V morphology of <22 mm may still be unsuitable for PPVI if the RVOT distends significantly at implantation, as stability cannot be assured. In practice, balloon sizing, performed at the time of catheterization, currently provides a 2D assessment of distensibility that can aid decision-making. In the future, this information could be derived non-invasively, with development of different CMR sequences, thus avoiding catheterization of patients who subsequently prove unsuitable for PPVI. Furthermore, our experience to date suggests that stent fractures are more commonly seen following PPVI in non-calcified outflow tracts or conduits (14). Again, this may be difficult to assess by MR angiography. Both the dynamic nature of the outflow tract and the wall thickness (consistent with calcification)

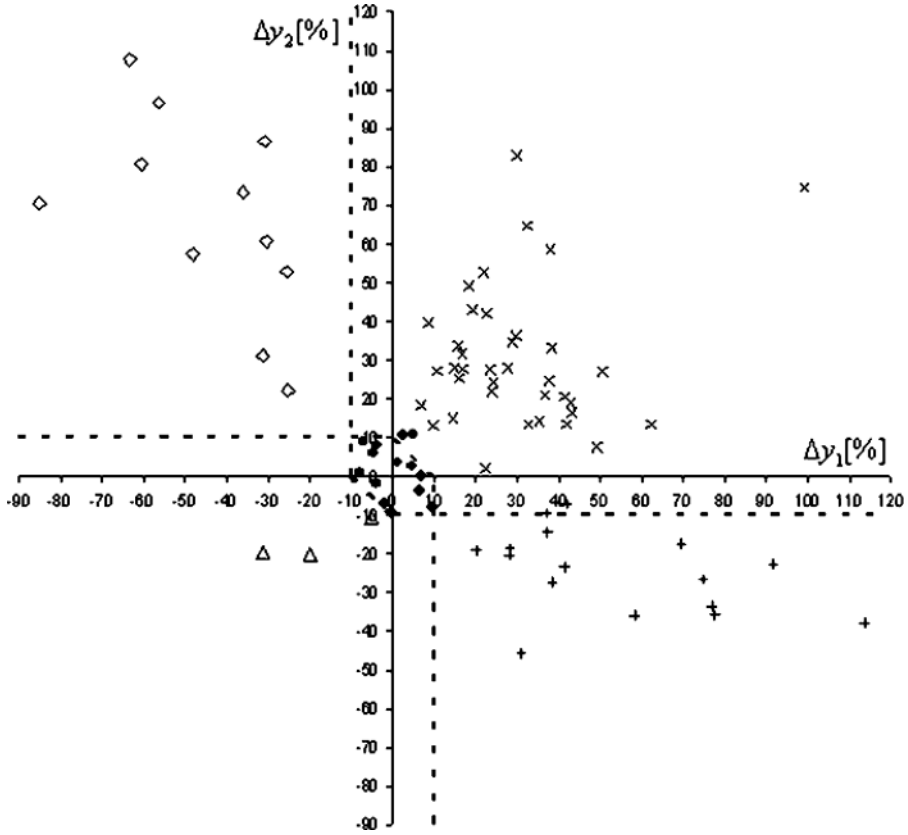

Figure 6. Distribution of the classifiable patients (n = 81) in the Δy1 Δy2 coordinate system. Four datasets, corresponding to patients who were wrongly assigned to their morphological type using visualization of 3D geometry alone, are out of their morphological type region.

may be assessed with gradient echo cine imaging trough the outflow tract or conduit.

Ninety-eight percent (81/83) of all morphologies could be described according to a simple three point system. Mathematical analysis of CMR data, therefore, has allowed us to optimize identification of the correct morphological sub-type and better select patients for PPVI. From this work, we have developed an algorithm that allows us to identify the morphological sub-group from the perimeter measurements at three levels in the RVOT, using commercially available MR software.

Type I morphology was associated with a higher pulmonary regurgitant fraction than other morphological sub-types. The detrimental effect of chronic pulmonary regurgitation on right ventricular function, exercise capacity and arrhythmia potential is well documented (2–4). Previous investigators have found a high pulmonary regurgitant fraction to be associated with the presence of a transannular patch (15) or a dilated pulmonary annulus (16). We would suggest that this is likely to be a consequence of the morphology of the RVOT that often develops following placement of a transannular patch. Fluid dynamics studies could provide an insight into the effect of different RVOT morphologies on the generation of pulmonary regurgitation and are an important area for future research. The clinical consequences of pulmonary regurgitation and the growing availability of new transcatheter treatments, however, have already influenced surgical approaches to primary repair. Thus, in our institution, there is a preference for placing smaller patches and where possible homograft conduits. It is most likely that, in the future, there will be fewer older patients seen with type I morphology and consequently a higher proportion suitable for PPVI.

Finally, although CMR is performed for all our patients referred with symptomatic RVOT dysfunction, our patient population may be biased. Though the exact percentages for each morphology may differ between different institutional practices, we believe that the 5 main morphologies we have described will be consistent.

Patient selection for PPVI on the basis of surgical history alone is not sufficient; 3D assessment of the RVOT with CMR and mathematical analysis provides important additional information. The type of morphology, in combination with RVOT size and distensibility, allows informed selection for the current generation of percutaneously implantable pulmonary valve devices. Detailed knowledge of these morphologies and understanding of distensibility will help us to design devices in the

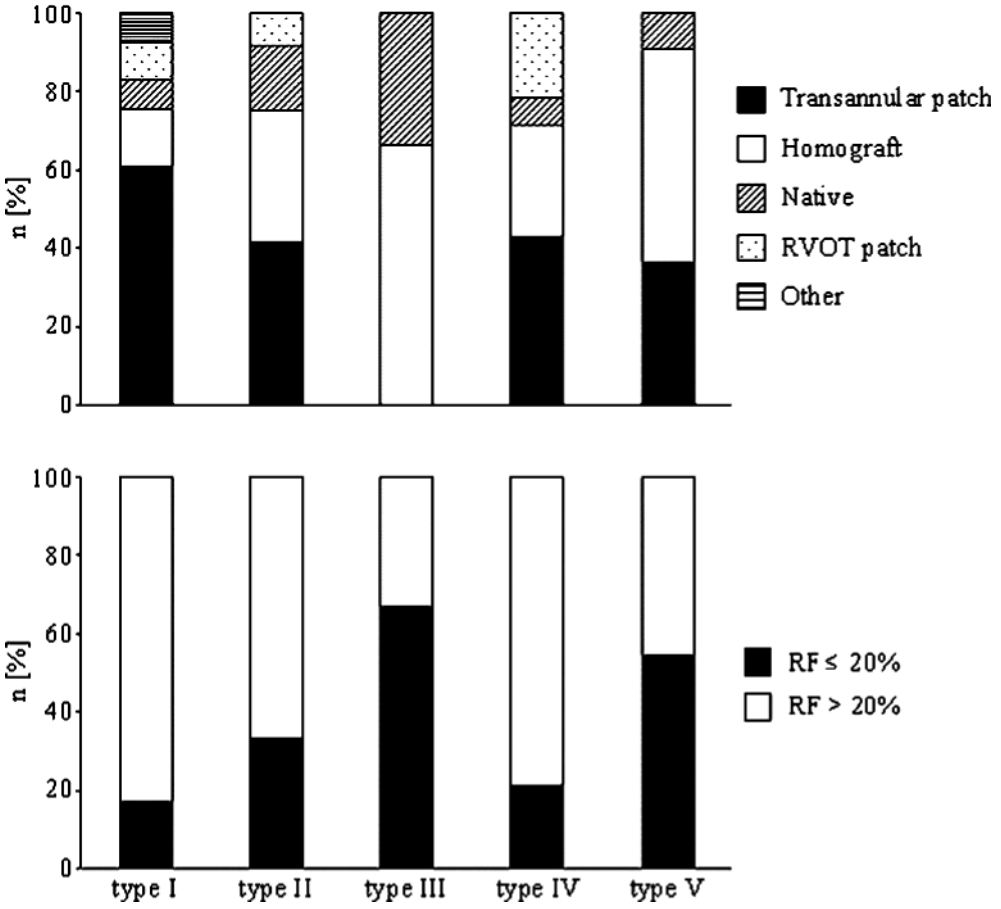

Figure 7. Distribution of a) outflow tract type and b) regurgitant fraction (RF) in the 5 morphological types (n = 81 classifiable patients, %).

future that will extend the indications to this growing patient population.

REFERENCES

1. Warnes CA, Liberthson R, Danielson GK, Dore A, Harris L, Hoffman JI, et al. Task force 1: The changing profile of congenital heart disease in adult life. J Am Coll Cardiol 2001;37:1170–5.
2. Bove EL, Byrum CJ, Thomas FD, Kavey RE, Sondheimer HM, Blackman MS, et al. The influence of pulmonary insufficiency on ventricular function following repair of tetralogy of Fallot. Evaluation using radionuclide ventriculography. J Thorac Cardiovasc Surg 1983;85:691–6.
3. Carvalho JS, Shinebourne EA, Busst C, Rigby ML, Redington AN. Exercise capacity after complete repair of tetralogy of Fallot: Deleterious effects of residual pulmonary regurgitation. Br Heart J 1992;67:470–3.
4. Gatzoulis MA, Balaji S, Webber SA, Sill SC, Hokanson JS, Poile C, et al. Risk factors for arrhythmia and sudden cardiac death late after repair of tetralogy of Fallot: A multicentre study. Lancet 2000;356:975–81.
5. Coats L, Khambadkone S, Derrick G, Sridharan S, Schievano S, Mist B, et al. Physiological and clinical consequences of relief of right ventricular outflow tract obstruction late after repair of congenital heart defects. Circulation 2006;113(17):2037–44.
6. Stark J, Bull C, Stajevic M, Jothi M, Elliott M, de Leval M. Fate of subpulmonary homograft conduits: Determinants of late homograft failure. J Thorac Cardiovasc Surg 1998;115(3):506–16.
7. Powell AJ, Lock JE, Keane JF, Perry SB. Prolongation of RV-PA conduit life span by percutaneous stent implantation. Intermediate-term results. Circulation 1995;92(11):3282–88.
8. Bonhoeffer P, Boudjemline Y, Qureshi SA, Le Bidois J, Iserin L, Acar P, et al. Percutaneous insertion of the pulmonary valve. J Am Coll Cardiol 2002;39(10):1664–9.
9. Khambadkone S, Coats L, Taylor A, Boudjemline Y, Derrick G, Tsang V, et al. Percutaneous pulmonary valve implantation in humans–Results in 59 consecutive patients. Circulation 2005;112(8):1189–97.
10. Choe YH, Kim YM, Han BK, Park KG, Lee HJ. MR imaging in the morphologic diagnosis of congenital heart disease. Radiographics 1997;17(2):403–22.
11. Taylor AM, Bogaert J. Cardiovascular MR imaging planes and segmentation. In: Bogaert J, Dymarkowski S, Taylor AM, eds. *Clinical Cardiac MRI*, 1st ed. Springer-Verlag, Berlin Heidelberg, 2005:85–98.
12. Schievano S, Migliavacca F, Coats L, Khambadkone S, Carminati M, Wilson N, et al. Planning of percutaneous pulmonary valve implantation based on rapid prototyping of the right ventricular outflow tract and pulmonary trunk from magnetic resonance imaging data. *Radiology* 2007. In press.
13. Boudjemline Y, Agnoletti G, Bonnet D, Sidi D, Bonhoeffer P. Percutaneous pulmonary valve replacement in a large right ventricular outflow tract: an experimental study. J Am Coll Cardiol 2004;43(6):1082–7.
14. Nordmeyer J, Khambadkone S, Coats L, Schievano S, Parenzan G, Taylor A, et al. Analysis of stent fractures after

percutaneous pulmonary valve implantation. Circulation 2006; 114(18):II-385.

15. Davlouros PA, Kilner PJ, Hornung TS, Li W, Francis TM, Moon JC, et al. Right ventricular function in adults with repaired tetralogy of Fallot assessed with cardiovascular magnetic resonance imaging: detrimental role of right ventricular outflow aneurysms or akinesia and adverse right-to-left ventricular interaction. J Am Coll Cardiol 2002;40(11):2044–52.

16. Uebing A, Fischer G, Bethge M, Scheewe J, Schmiel F, Stieh J, et al. Influence of the pulmonary annulus diameter on pulmonary regurgitation and right ventricular pressure load after repair of tetralogy of Fallot. Heart 2002;88(5):510–4.